

Strong and Selective Ni(II) Extractants Based on Synergistic Mixtures of Sulfonic Acids and Bidentate N-Heterocycles

Roebuck, J. W.; Bailey, P. J.; Doidge, E. D.; Fischmann, A. J.; Healy, M. R.; Nichol, G. S.; O'Toole, N.; Pelser, M.; Sassi, T.; Sole, K. C.; Tasker, P. A.;

Originally published:

November 2018

Solvent Extraction and Ion Exchange 36(2019)5, 437-458

DOI: <https://doi.org/10.1080/07366299.2018.1506558>

Perma-Link to Publication Repository of HZDR:

<https://www.hzdr.de/publications/Publ-28983>

Release of the secondary publication
on the basis of the German Copyright Law § 38 Section 4.

Strong and Selective Ni(II) Extractants Based on Synergistic Mixtures of Sulfonic Acids and Bidentate N-Heterocycles

James W. Roebuck^a, Philip J. Bailey^a, Euan D. Doidge^a, Adam J. Fischmann^b, Mary R. Healy^a, Gary S. Nichol^a, Niall O'Toole^a, Max Pelsler^c, Thomas Sassi^b, Kathryn C. Sole^c, and Peter A. Tasker^a

^aEaStCHEM School of Chemistry, University of Edinburgh, Edinburgh, UK; ^bSolvay Technology Solutions, Metal Extraction Products, Stamford, CT, USA; ^cAnglo American Technical Solutions, Johannesburg, South Africa

ABSTRACT

Bidentate 5,5'-alkyl-3,3'-bi-1H-pyrazole and 2-(5-alkyl-1H-pyrazol-3-yl)pyridine ligands, L^5 and L^6 , have been shown to be stronger synergists for the solvent extraction of Ni(II) from sulfate solutions by dinonylnaphthalene sulfonic acid (DNNSAH) than the structurally related tridentate ligand 2,6-bis-[5-*n*-nonylpyrazol-3-yl]pyridine, L^1 , previously reported by Zhou and Pesic. The bidentate ligands are highly selective, providing the option of sequential recovery of Ni(II) and Co(II) and rejection of other metals commonly found in the liquors resulting from the acidic sulfate leaching of laterite ores. They were the strongest synergists identified in a screening carried out on 18 types of bidentate and tridentate N-heterocyclic ligands, including the recently reported 2-(2'-pyridyl)imidazoles, L^{9-11} . X-ray crystal structures of Ni(II) complexes of model ligands for L^5 and L^6 , having *t*-butyl rather than long-chain alkyl groups and with 2-naphthalene sulfonate rather than DNNSA⁻ as counteranions, show that the $[Ni(L)_3]^{2+}$ complexes form strong H-bonds from the pyrazolyl NH groups to the oxygen atoms of the sulfonate groups, an arrangement that will stabilize $[Ni(L)_3 \cdot (DNNSA)_2]$ assemblies and shield their polar functionalities from diluent molecules of the water-immiscible phase. UV-visible spectra and mass spectrometry provide evidence for the strong synergists displacing all water molecules from the inner coordination sphere of the Ni(II) ions.

Keywords

Ni recovery; laterite processing; synergistic solvent extraction; outer-sphere bonding; supramolecular chemistry

Introduction

There is considerable interest in developing processes to recover nickel and cobalt efficiently from nickeliferous laterites, which constitute approximately 60%–70% of total nickel resources worldwide.^[1,2] Surface lateritic deposits, such as limonites, typically have less than 2% nickel and relatively low concentrations of MgO, with high moisture and iron contents, so they are not well suited to pyrometallurgical smelting processes^[3] that are commonly used for nickel recovery from silicate lateritic and sulfidic ores.^[4–8] Development of the Caron process has been commercially applied in several operations,^[7–9] but none ever operated very profitably; the process is highly energy- and reagent-intensive (for drying, reductive roasting, and ammoniacal leaching) and achieves relatively low nickel recoveries of about 80%.^[1] Limonitic laterites can also be processed by high-pressure acid leaching (HPAL), but downstream recovery of nickel from the resulting sulfate streams is currently not very efficient. It requires the pH to be raised to precipitate iron(III) as an oxyhydroxide waste. The Ni(II) extractants used to date do not have the strength or selectivity to provide efficient separation from other metals,^[10] are very soluble in the aqueous

phase,^[10,11] or are unstable and readily poisoned by trace impurities.^[12] More recently a nitric acid leaching process has been proposed,^[13] in which the phosphinic-acid extractant CYANEX 272 would be used to separate aluminum, cobalt, and nickel from each other.

One of the most promising approaches to the recovery of nickel and cobalt from HPAL circuits involves synergistic solvent extraction, the concept of which was originally proposed by Preston and coworkers.^[14–18] Much of the work in this area focused on mixtures of hydrophobic carboxylic acids and either pyridinecarboxylate esters or α -hydroxyoximes and was directed at increasing the Ni(II) extraction strength of such synergistic mixtures,^[15,19–22] improving stability of the oximes toward hydrolysis,^[23–26] and increasing the retention of the carboxylic acid component in hydrocarbon diluents. Use of the NickSyn™ system (a synergistic combination of Versatic 10 and a proprietary pyridine carboxylate) has been piloted.^[27–30]

Studies of the mechanism of extraction suggest that hydrogen bonding between the two types of extractants (see Fig. 1) helps to stabilize the Ni complexes formed in the water-immiscible phase.^[24,32] Incorporating such design features, which essentially exploit H-bonding in the outer coordination sphere, is central to the work described in this article. It aims to use combinations of neutral bidentate heterocyclic ligands and sulfonic acids to generate strong extractants for Ni(II) that could find use in HPAL processing of laterites. In the longer term, it would be beneficial if such new strong extractants could also be used in novel flowsheets to provide better materials balances for laterite processing.

The dominant component (40%–50%) of typical limonite ores is iron, so there is an economic incentive to develop commercial-scale processes that recover iron as a saleable by-product. Such a product would improve HPAL-type processes by eliminating the major waste stream, as well as providing an additional

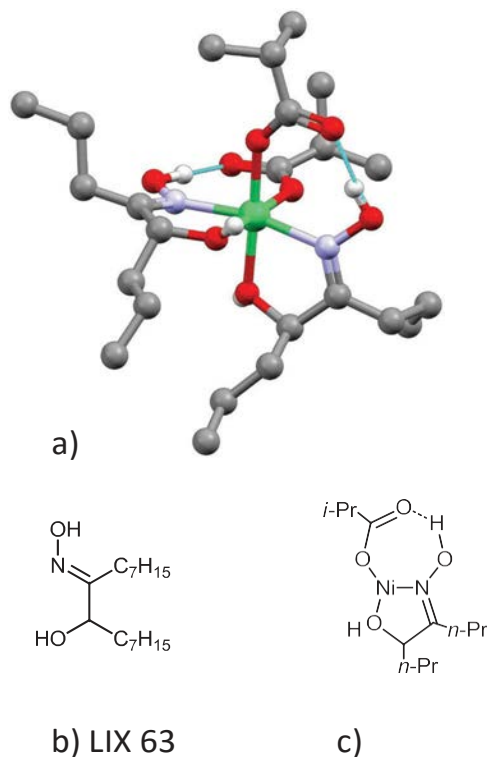


Figure 1. (a) Interligand H-bonding between the oxime OH group and a carboxylate oxygen atom in the X-ray crystal structure of $[\text{Ni}(n\text{-Pr-hydroxyoxime})_2(i\text{-Pr-COO})_2]$,^[32] a model for complexes extracted by synergistic mixtures of (b) LIX 63 and Versatic 10, showing (c) the pseudo-tridentate ligand present.

source of revenue.^[3] Several regenerative atmospheric leaching processes, such as the Anglo Research Nickel (ARNi) process, have the potential to greatly reduce capital costs,^[31,33] but the Anglo Research Iron (ARFe) flowsheet (Fig. 2) also generates hematite as a saleable by-product. In this type of circuit, nickel and cobalt are recovered by precipitation as a mixed-metal sulfide as an intermediate product for further processing.^[33,34]

Using solvent extraction to effect the removal and recovery of these metals at the same point in the circuit is considered in this article. At the outset, it was assumed that existing Ni extractants would not meet the requirements of such a circuit but, as in HPAL flowsheets,^[35] it might be practicable to use phosphinate extractants, such as CYANEX 272, to recover cobalt efficiently.

If a very strong extractant was available that showed high selectivity over iron, it might also be possible to recover nickel earlier in the flowsheet *before* the crystallization step in the ARFe process. Such an approach would be analogous to that used in the commercially successful leach/solvent extraction/electrowinning of copper, which currently accounts for ca. 20% of copper production worldwide.^[36-41]

The starting point for the work described below was the report in 1997^[42] that the addition of 2,6-bis-[5-*n*-nonylpyrazol-3-yl]pyridine (L^1 in Table 1) to dinonylnaphthalene sulfonic acid (DNNSAH) lowered the $pH_{1/2}$, the pH at which half of the Ni(II) in a sulfate feed solution is extracted, by more than two pH units and potentially provided a reagent that could sequentially recover Ni(II) and Co(II) from laterite feed solutions containing Fe(II) and Fe(III). Using synergists to enhance the performance of DNNSAH is similar to the tactic employed by Grinstead,^[43] who showed that a range of substituted pyridines, particularly picolinic esters and amides, substantially increased distribution ratios for Ni transfer from sulfate solutions. Surprisingly, there have been no reports of attempts to apply the DNNSAH/ L^1 system to the recovery of nickel from pregnant leach solutions (PLSs) derived from laterites, possibly because the triheterocyclic structure of L^1 is likely to make it costly to

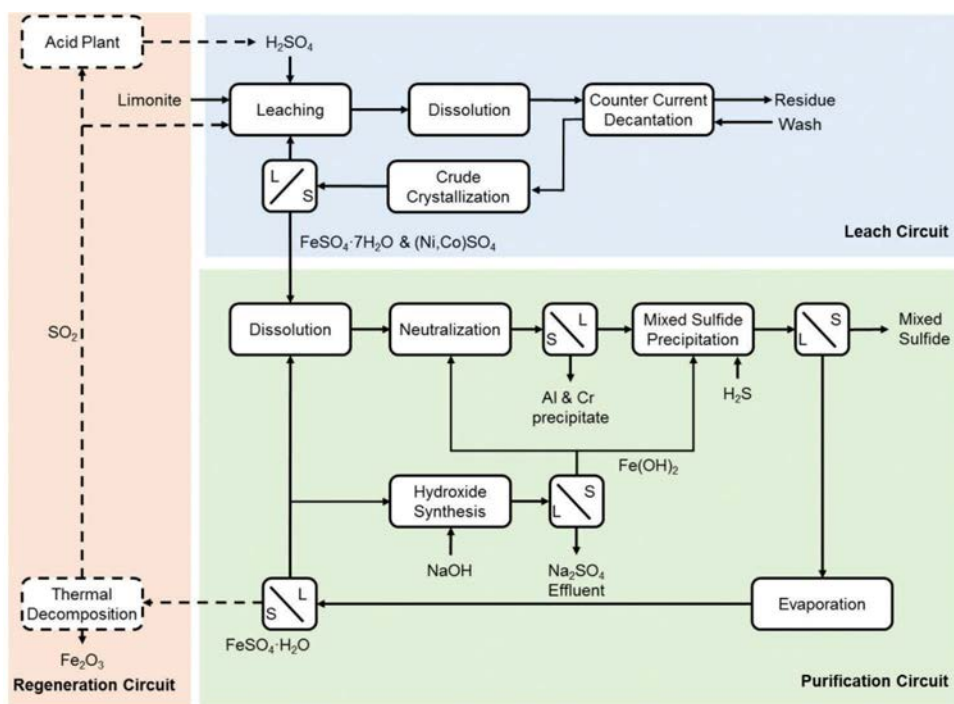
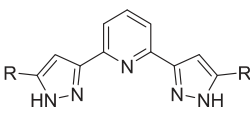

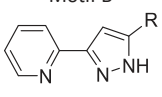

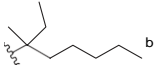
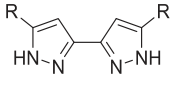

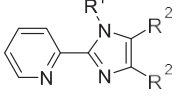
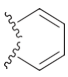


Figure 2. Flow diagram showing the regenerative leach approach of the ARFe process^[3] and the routing of iron to a saleable product (hematite) rather than to a waste stream.

Table 1. Bidentate ligands L²⁻⁸ selected in the first phase of the program for evaluation as potential synergists for Ni extraction by DNNSAH, showing their structural relationship to the effective extractants: 2,6-bis-[5-*n*-nonylpyrazol-3-yl]pyridine (L¹)^[42] and 1-alkyl-2-(2'-pyridyl)imidazoles (L⁹⁻¹¹)^[44]

Motif	R	L [#]	pH _{1/2} Ni	pH _{1/2} Co	Diluent, notes, and source	
Motif A 	<i>n</i> -C ₉ H ₁₉	L ¹	-0.7	-0.5	Kermac 470B ^[42] (this work)/CHCl ₃	
		L ²	-	-	Model for L ¹	
Motif B 		L ³	-	-	Model for L ⁴⁻⁵	
		L ⁴	<0 ^a	0.75	ORFOM SX-12 ^[44]	
	<i>n</i> -C ₉ H ₁₉	L ⁵	-1.1	-0.5	CHCl ₃	
Motif C 	<i>n</i> -C ₉ H ₁₉	L ⁶	-0.7	0.1	toluene	
		L ⁷	-	-	Model for L ⁶	
Motif D 	R ¹ : <i>i</i> Pr	R ² : 	L ⁸	-	-	Model for L ⁹⁻¹¹
	<i>n</i> -C ₇ H ₁₅	H	L ⁹	1.5 ^c	-	2-octanol + Shellsol 2325 (8:2) ^[44]
	<i>n</i> -C ₈ H ₁₇	H	L ¹⁰	1.4 ^c	3.0 ^c	2-octanol + Shellsol 2325 (8:2) ^[44]
	<i>n</i> -C ₁₀ H ₂₁	H	L ¹¹	1.5 ^c	2.5 ^c	2-octanol + Shellsol 2325 (8:2) ^[44]

^aA full S-curve was not determined. At pH 0, the loading was 68%.

^bOther isomers were present because Versatic 10 was used as a precursor.

^cValue estimated from S-curves in Okewole *et al.*^[44].

manufacture. In seeking simpler synergists for DNNSA⁻ that might also greatly increase its strength as a Ni extractant, we used the hypothesis that the Ni(II) complexes of L¹ form favorable H-bonded assemblies with the sulfonate group on DNNSA⁻ in the outer coordination sphere (a possible arrangement involving two-fold symmetry is shown in Fig. 3(a)). Such an assembly contrasts with those that might account for the synergism shown by carboxylate/hydroxyoxime systems (see Fig. 1) because the anionic component does not enter the inner coordination sphere of the Ni(II) atom. The

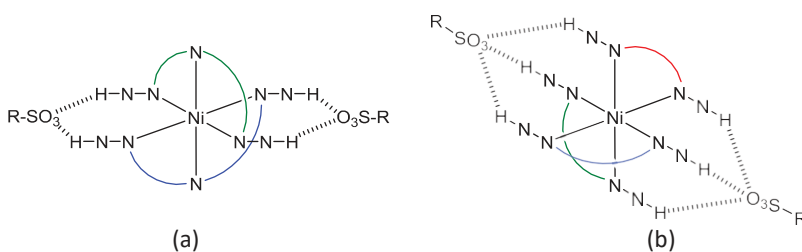


Figure 3. Representations of the possible H-bonding between DNNSA⁻ and the N-H groups in the outer coordination spheres of Ni(II) in neutral assemblies formed by (a) the tridentate synergists L¹ and L² and (b) bidentate analogues L³⁻⁸.

hypothesis that favorable outer-sphere H-bonding by the *tridentate* ligand L¹ might enhance the stability of [Ni(L¹)₂][DNNSA]₂ assemblies was tested by synthesizing *bidentate* analogues, L³-L⁷, which would also present arrays of pyrazole NH groups in the outer spheres of [Ni(L)₃]²⁺ complexes and could form strong hydrogen bonds to the oxygen atoms in the DNNSA⁻ anion (see Fig. 3(b)).

Shortly after work commenced, a paper appeared^[44] that demonstrated that the 2-(2'-pyridyl)-imidazoles, L⁹⁻¹¹, are very effective in enhancing the strength of Ni extraction by DNNSAH. These ligands do not contain strong NH hydrogen-bond donor groups. The screening of potential synergists was consequently extended to allow comparison of bidentate N-heterocyclic ligands having similar chemical compositions, some with and some without strong H-bond donor groups (see L¹²⁻³⁹ in Table 2), to establish to what extent H-bonding stabilizes ion pairs formed in the water-immiscible phase and increases the strength of Ni extraction.

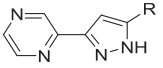
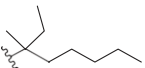
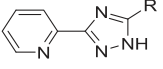
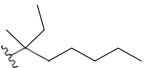
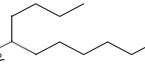
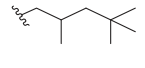
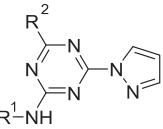
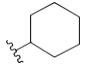
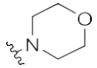
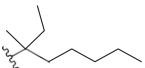
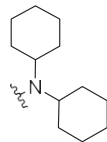
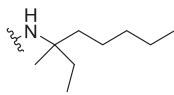
Experimental

All solvents and reagents were used as received from Sigma-Aldrich, Fisher Scientific UK, VWR International, Merck, or Alfa Aesar. Toluene and tetrahydrofuran were dried by passage-activated alumina columns using a solvent purification system and used immediately for synthesis. Flash chromatography was carried out with silica gel using Still's method.^[45] ¹H and ¹³C nuclear magnetic resonance spectra were recorded at 298 K on Bruker AVA600, AVA500, or AVA400 spectrometers as CDCl₃ or DMSO-d₆ solutions. Chemical shifts are reported in δ (ppm) relative to residual solvent (δ_{H} 7.26 and δ_{C} 77.0 or δ_{H} 2.50 and δ_{C} 39.5). Elemental (C, H, and N) micro-analyses were carried out by Mr. Stephen Boyer at London Metropolitan University, School of Human Sciences, 29, Hornsey Road, London, N7 7DD.

Mass spectra were recorded on Thermo-Fisher LCQ Classic electrospray ionization (ESI) or Thermo Electron MAT 900 XP electron ionization (EI) spectrometers. ESI Fourier Transform ion cyclotron resonance mass spectra (FT-ICR MS) measurements were recorded in positive-ion mode using the standard Bruker ESI sprayer operated in "infusion" mode coupled to a Solarix FT-ICR mass spectrometer. Direct infusion spectra were typically a sum of 20 acquisitions. All mass spectra were analyzed using DataAnalysis software version 4.4 (Bruker Daltonics). Ions were assigned manually.

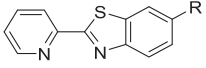
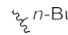
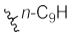
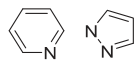
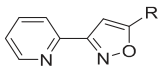
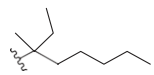
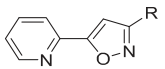
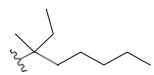
At the University of Edinburgh, inductively coupled plasma optical-emission spectroscopy (ICP-OES) was carried out using a Perkin Elmer 5300DV spectrometer. 1-Methoxy-2-propanol solutions were taken up with a peristaltic pump into a Gem Tip cross-flow nebulizer and a Glass Cyclonic spray chamber at a rate of 2.0 mL min⁻¹. Torch settings used a radio-frequency forward power of 1500 W and argon gas flows of 20, 1.4, and 0.45 L min⁻¹ for plasma, auxiliary, and nebulizer flows, respectively. Data were processed using WinLab32 version 3.0.0.0103. In the Solvay laboratories, an Agilent Vista-Pro ICP-OES was used for aqueous samples (diluted in 2% v/v HNO₃) and an Agilent MP-4100 instrument for solutions in organic solvents, which were

Table 2. Structures of potential synergists for Co(II) and Ni(II) extraction by DNSSAH with $\text{pH}_{1/2}$ values for recovery from sulfate solutions.

Motif	R group	L [#]	$\text{pH}_{1/2}$ Ni	$\text{pH}_{1/2}$ Co	Diluent; pH range for extraction(s); loadings at specific pH values; other metals extracted; notes
Motif E 		L ¹²	<0 ^a	<0.5	ORFOM® SX-12; pH 0-1.6; 68% Ni at pH 0
Motif F 		L ¹³	<0 ^a	1.3	ORFOM® SX-12; pH 0-1.6; 91% Ni at pH 0
		L ¹⁴	-	-	ORFOM® SX-12; formed ppt.
		L ¹⁵	-	-	ORFOM® SX-12; formed ppt.
Motif G 	R ¹ 	R ² 	L ¹⁶	< 0 ^a	0.6 ORFOM® SX-12; pH 0-1.2; 91% Ni at pH 0
			L ¹⁷	<1.3 ^a	<1.3 ^a ORFOM® SX-12; pH 1.3; 72% Ni and 87% Co at pH 1.3; Cu, Zn, Mn ^b
	R ¹ = R ² 		L ¹⁸	<1.6 ^a	<1.6 ^a ORFOM® SX-12; pH 1.6; 58% Ni and 75% Co at pH 1.6; Cu, Zn ^b

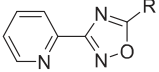
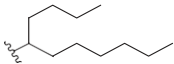
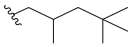
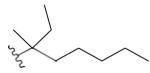
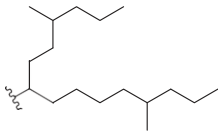
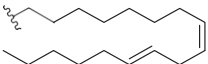
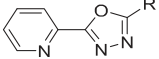
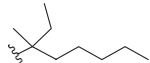
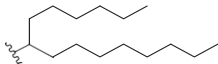
(Continued)

Table 2. (Continued).

Motif	R group	L [#]	pH _½ Ni	pH _½ Co	Diluent; pH range for extraction(s); loadings at specific pH values; other metals extracted; notes
<p>Motif H</p> 	<p><i>n</i>-Bu</p> 	L ¹⁹	-	-	Model ligand, not used for SX
	<p><i>n</i>-C₉H₁₉</p> 	L ²⁰	0.0	0.6	CHCl ₃ ; for selectivity, see experimental section
<p>Motif I</p> 	N/A	L ²¹	<0 ^a	<0 ^a	CHCl ₂ CHCl ₂ ; pH 0–1.4; 99% Ni and 68% Co at pH 0; Al, Cr
<p>Motif J</p> 		L ²²	>1.5 ^a	>1.5 ^a	ORFOM®SX-12; pH 0–1.3; 28% Ni and 7% Co at pH 1.3; Mn, Mg
<p>Motif K</p> 		L ²³	>2 ^a	>2 ^a	ORFOM®SX-12; pH 0–1.9; 28% Ni and 7% Co at pH 1.9; Mn, Mg, Fe

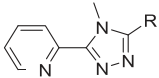
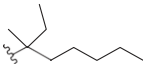
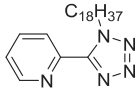
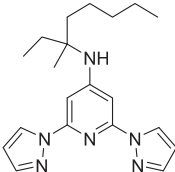
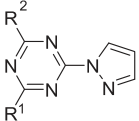
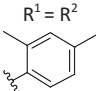
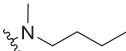
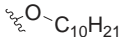
(Continued)

Table 2. (Continued).

Motif	R group	L [#]	pH _{1/2} Ni	pH _{1/2} Co	Diluent; pH range for extraction(s); loadings at specific pH values; other metals extracted; notes
Motif L 		L ²⁴	<1.2 ^a	2	ORFOM®SX-12; pH 1.2-2.7; 69% Ni at pH 1.2; Zn, Cu
		L ²⁵	< 0 ^a	1.2	ORFOM®SX-12; pH 0-2.1; 76% Ni at pH 0; Cu, Zn, Mn
		L ²⁶	1.5	>2	ORFOM®SX-12; pH 0.6-1.8; 62% Ni and 35% Co at pH 1.8; Cu, Zn
		L ²⁷	<0 ^a	1.2	ORFOM®SX-12; pH 0-1.7; 76% Ni at pH 0; Cu, Zn
		L ²⁸	<1.3 ^a	>1.3 ^a	ORFOM®SX-12; pH 1.3; 89% Ni and 39% Co at pH 1.3; Cu, Zn
Motif M 		L ²⁹	<1.0 ^a	ca 1.9 ^a	ORFOM®SX-12; two pHs used: 87% Ni and 31% Co at pH 1.4 and 94% Ni and 51% Co at pH 1.9; Cu, Zn
		L ³⁰	<1.3 ^a	>1.3 ^a	ORFOM®SX-12; pH 1.3; 93% Ni and 28% at pH 1.3; Co Cu, Zn ^b

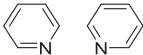
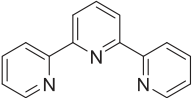
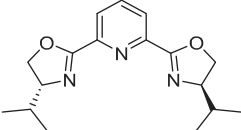
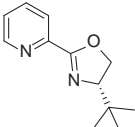
(Continued)

Table 2. (Continued).

Motif	R group	L [#]	pH _{1/2} Ni	pH _{1/2} Co	Diluent; pH range for extraction(s); loadings at specific pH values; other metals extracted; notes	
<p>Motif N</p>  <p>(mixture of three isomers with Me on other N atoms of triazole)</p>		L ³¹	>2.1 ^a	>2.1 ^a	ORFOM®SX-12; pH 0.8-2.1; 41% Ni and 20% Co at pH 2.1; Cu, Zn, Al, Cr, Mg, Mn	
<p>Motif O</p> 	<p>1-octyl isomer (shown)</p> <p>3-octyl isomer</p>	L ³²	<-0.1 ^a	1.25	CHCl ₂ CHCl ₂ ; pH -0.1 - 1.50; 52% Ni at pH -0.1; 67% Ni at pH 0; 16% Co at pH 2	
<p>Motif P</p> 	N/A	L ³³	<1.3 ^a	>1.3 ^a	ORFOM®SX-12; pH 1.3; 73% Ni and 46% Co at pH 1.3; potentially tridentate; Cu, Zn, Ca ^b	
<p>Motif Q</p> 	 <p>R¹ = R²</p>	L ³⁴	< 0 ^a	0.2 ^a	ORFOM®SX-12; pH 0-1.7; 72% Ni at pH 1.3; Mg	
	<p>R¹</p> 	<p>R²</p> 	L ³⁵	< 1.2 ^a	> 1.2 ^a	ORFOM®SX-12; pH 1.2; 79% Ni and 44% Co at pH 1.2; Cu ^b

(Continued)

Table 2. (Continued).

Motif	R group	L [#]	pH _{1/2} Ni	pH _{1/2} Co	Diluent; pH range for extraction(s); loadings at specific pH values; other metals extracted; notes
Motif R 	N/A	L ³⁶	<0.7 ^a	>1.5 ^a	Toluene; pH 0.7–1.5; 91% Ni at pH 0.7 and 24% Co at pH 1.5; Fe
Motif S 	N/A	L ³⁷	<0.8 ^a	>1.6 ^a	Toluene; pH 0.8–1.6; 79% Ni at pH 0.8 and 6% Co at pH 1.6; potentially tridentate; Fe
Motif T 	N/A	L ³⁸	>2 ^a	>2 ^a	Toluene; pH 0.8–2.0; 7% Ni and 6% Co at pH 1.6; potentially tridentate; Fe
Motif U 	N/A	L ³⁹	>2 ^a	>2 ^a	Toluene; pH 0.8–2.0; 9% Ni and 8% Co at pH 2.0; Fe

^aThese values are derived from an incomplete S-curve or from a single extraction point at the specified pH, and Ni-loadings are recorded in the right-hand column. ^bFor these extractions, the aqueous feed solution also contained Cu(II) and Zn(II) at the same concentration.

diluted in Premisolv and calibrated using Conostan metallo-organic standards (both from SCP Science, Quebec, Canada).

Single-crystal X-ray diffraction measurements were carried out on a Rigaku Oxford Diffraction SuperNova using Mo or Cu K α radiation. The crystal temperature was kept constant at either 100 or 120 K with an Oxford Cryosystems Cryostream. Data for five structures have been deposited with the Cambridge Crystallographic Data Centre with deposition numbers as follows: 1541479, [Co(L²)₂][ClO₄]₂·2MeOH; 1541480, [Ni(L²)₂][ClO₄]₂·H₂O·MeOH; 1541481, [Ni(L³)₃·(2-naphth-SO₃)₂]; 1541482, [Ni(L⁷)₃·(2-naphth-SO₃)₂]; and 1541483, [Ni(L²)₂·(2-naphth-SO₃)₂]. The last complex was isolated as a solvate, [Ni(L²)₂·(2-naphth-SO₃)₂]*n*CHCl₃, which lost chloroform and gave an X-ray diffraction pattern characteristic of a modulated structure. Processing of the data for this structure is described in a detailed report in the SI.

Ligand synthesis

Ligands L¹ and L⁹⁻¹¹ were prepared as described previously.^[42,44] Synthetic details for all other ligands are provided in the ESI.

Extraction procedures

pH dependence of metal extraction by DNNSAH and L¹

A mixed-metal stock solution was prepared with Fe(II), Co(II), and Ni(II) as their sulfate salts (0.2 g L⁻¹ of each metal) in sulfuric acid (30 g L⁻¹). The pH values prior to extraction were varied by diluting the stock solution (1.25 mL) with sodium hydroxide (1.25 mL, 5–75 mM) or sulfuric acid (1.25 mL, 5–12 mM) and making up to 5.0 mL. Extractions were carried out by contacting 2.5 mL chloroform solutions of L¹ (10 mM) and DNNSAH (10 mM) with mixed-metal stock solutions (2.5 mL) in sealed 7-mL vials with stirrer bars. After stirring at 1000 rpm for 22 h, the vials were centrifuged for 5 min, and 0.5 mL samples of each organic phase were evaporated to dryness and dissolved in 1-methoxy-2-propanol (10.0 mL). An ICP multi-element standard VI (Merck) was used to prepare standard solutions (1–10 mg L⁻¹ of Fe, Co, and Ni). The concentration of the metals was determined *via* ICP-OES from intensities measured at wavelengths of 221.648 (Ni), 231.160 (Co), and 239.562 (Fe) nm. Reported pH_{1/2} values are based on the concentration of metal in the chloroform phase (estimated error $\leq 5\%$ of theoretical maximum, 100%) relative to the total in the extraction experiment. The equilibrium pH values were determined *via* titration of samples (0.5 mL) of the aqueous phases against sodium hydroxide solutions (10 mM or 1 mM).

pH dependence of metal extraction by DNNSAH and L⁵, L⁶, L⁸, or L²⁰

Extractions were carried out using the procedure described above, but the concentrations of DNNSAH and the synergists (Lⁿ) used were dependent on the solubilities of the synergists and the quantities available (see ESI, section 2). Zn(II) was also included in the mixed-metal (sulfate) aqueous phase at the same concentration as the other metals.

Screening of selectivity and pH_{1/2} values for Ni(II) and Co(II) extraction of potential synergists listed in Table 2

Aqueous solutions PLS1 and PLS2 (modeling PLSs) with the compositions shown in Table 3 were prepared from the listed reagent-grade salts. The pH was adjusted to 3.0 (for PLS1) and 1.0 (for PLS2) by addition of sulfuric acid. Extractant solutions contained 0.185 M DNNSAH and 0.28 M of the potential synergist in ORFOM SX-12. Aliquots of the organic phase (5.5 mL) were mixed with portions of one of the PLS compositions in Table 3 (5.0 mL) and 0.5 mL of H₂SO₄ solution, water, or

Table 3. Compositions of solutions used as models for Ni laterite PLSs. Concentrations V_M of the metals are given in mg L^{-1} , where $V_M = m_M/V_S$, V_S being the volume of the solution, and m_M being the mass of the metal.

Element	PLS1	PLS2	Source
Ni	5000	5000	$\text{NiSO}_4 \cdot 6\text{H}_2\text{O}$
Co	500	500	$\text{CoSO}_4 \cdot 7\text{H}_2\text{O}$
Mn	1500	2900	$\text{MnSO}_4 \cdot \text{H}_2\text{O}$
Mg	15 000	15 000	MgSO_4
Zn	100	200*	$\text{ZnSO}_4 \cdot 7\text{H}_2\text{O}$
Ca	500	0	CaCl_2
Na	2800	0	NaCl
Fe	20	3200	$\text{Fe}_2(\text{SO}_4)_3 \cdot 7\text{H}_2\text{O}$
Si	15	0	$\text{Na}_3\text{SiO}_4\text{H}$ (solution)
Al	0	200	$\text{Al}_2(\text{SO}_4)_3 \cdot 16\text{H}_2\text{O}$
Cr	0	100	$\text{Cr}_2(\text{SO}_4)_3 \cdot x\text{H}_2\text{O}$
Cu	200	200*	$\text{CuSO}_4 \cdot 5\text{H}_2\text{O}$
pH	3	1	H_2SO_4

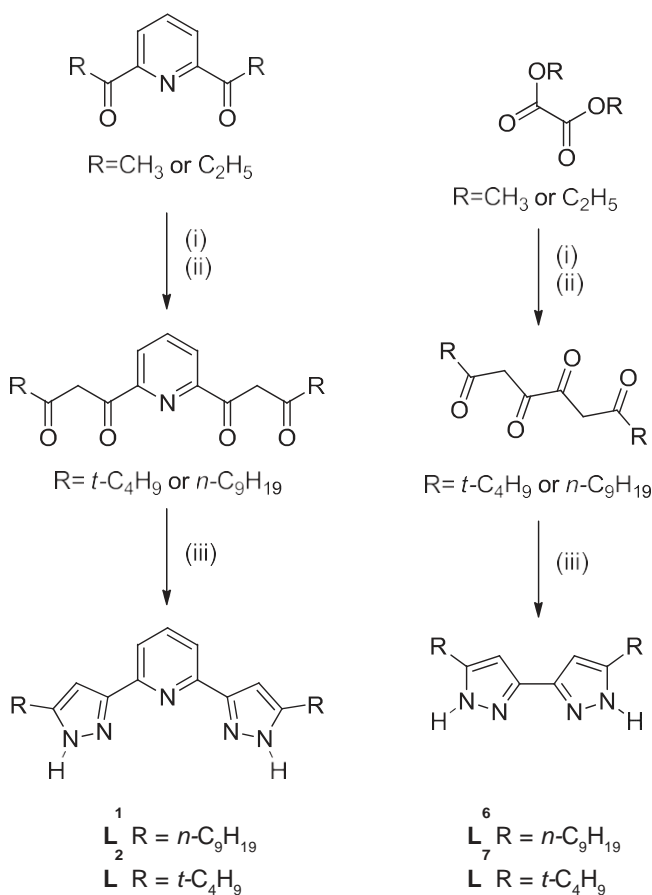
NaOH solution to obtain a range of final pH values after stirring for at least 2 h. The phases were separated and filtered (the organic phases through Whatman 1PS phase separating paper and the aqueous phases through Whatman 1 filter paper), and the metal content of each was analyzed by ICP for the aqueous phase and by microwave plasma atomic emission spectrometry for the organic phase. The $\text{pH}_{1/2}$ (the value of pH where the metal ion under consideration is equally distributed between aqueous and organic phases) was measured from a plot of extraction *vs.* pH.

Results and discussion

Samples of the previously reported^[42] ligand, 2,6-bis-[5-*n*-nonylpyrazol-3-yl]pyridine, L^1 , and a model, L^2 , with *t*-butyl groups replacing its two *n*-nonyl groups were prepared by treating diesters of pyridine-2,6-dicarboxylic acid under strongly basic conditions with undecanone or pinacolone, followed by reaction with hydrazine hydrate (See Scheme 1 and ESI). Similar routes were used to prepare the *mono*-pyrazol-3-yl ligands, L^{3-5} ,^[46] based on syntheses of related compounds by others.^[47] The tetraketone precursors for L^6 and L^7 were prepared by reaction of undecanone or pinacolone with diethylxalate (Scheme 1 and ESI) in the presence of sodium hydride and the N-alkylimidazoles L^{8-11} , as described by Okewole *et al.*^[44] Synthetic details for all other ligands used in this work, L^{12-39} , have been reported in a patent application.^[46] Some additional information is provided in the ESI, including a cross-referencing of compound numbers with those used in this article.

The tightly bunched S-curves observed for DNNSAH extraction of Cu(II), Co(II), Ni(II), Mn(II), Zn(II), and Mg(II) as a function of pH ($\text{pH}_{1/2}$ values fall in the range 1.7–2.3 in Shellsol A), separated considerably and shifted to much lower pH values when an equimolar amount of the bis-pyrazolyl ligand L^1 was added to a solution DNNSAH in Kermac 47B (0.05 M).^[42] Very similar behavior was observed in this work with a chloroform solution containing 0.03 M L^1 and DNNSAH (Fig. 4). These results confirm that an L^1 /DNNSAH mixture could be used to separate Ni(II) and Co(II) from Fe(II), a key requirement for the new flowsheets to process lateritic ores described in the Introduction.

In seeking simpler, lower-cost alternatives to L^1 to enhance the strength and selectivity of DNNSAH extraction of Ni, it is helpful to know the mode of action of the L^1 /DNNSAH mixture. Given the weakly coordinating nature of organic sulfonates and the proposition^[48] that base-metal extraction by DNNSAH alone involves a reverse-micelle mechanism in which the metal cations retain water in their inner coordination spheres, it is likely that two strongly coordinating L^1 tridentate ligands will define the inner coordination sphere of the Ni atom and that ion-paired assemblies $[\text{Ni}(L^1)_2 \cdot (\text{DNSSA})_2]$ will be present in the water-immiscible solvent. For this work, we assumed that some forms of hydrogen bonding between the NH groups of the pyrazole units in L^1



Scheme 1. Routes (i) $n\text{-C}_9\text{H}_{19}\text{COCH}_3$ or $t\text{-C}_4\text{H}_9\text{COCH}_3$, (ii) NaH or NaOCH_3 and (iii) $\text{NH}_2\text{NH}_2 \cdot \text{H}_2\text{O}$ to the bis-pyrazolyl ligands L^1 , L^2 , L^6 , and L^7 via the appropriate tetraketonones. Full experimental details can be found in the ESI.

and the oxygen atoms of the sulfonate groups could stabilize the assemblies and enhance Ni extraction.

Attempts to isolate high quality crystals of a model complex, $[\text{Ni}(\text{L}^2)_2 \cdot (2\text{-naphth-SO}_3)_2]$, in which *t*-butyl groups replaced the *n*-nonyl groups in L^1 and 2-naphthalene sulfonate was used as the counter-anion instead of DNNSA^- , proved difficult. Crystals of a solvate, $[\text{Ni}(\text{L}^2)_2 \cdot (2\text{-naphth-SO}_3)_2] \cdot n\text{CHCl}_3$, rapidly lost chloroform immediately upon removal from the mother liquor prior to data collection, resulting in partial crystal decomposition. When a suitable crystal was eventually mounted on the diffractometer, it gave an X-ray diffraction pattern characteristic of a modulated structure. The treatment of data for this structure is described in a detailed report in the SI. Despite it proving impossible to define the positions of many of the carbon atoms in the 2-naphthalene sulfonate ions based on difference Fourier electron density maps, the $[\text{Ni}(\text{L}^2)_2]^{2+}$ complex units had the expected pseudo-octahedral structures similar to those found in other salts (see below). It is also clear that all pyrazole N-H groups make close contacts with sulfonate oxygen atoms, with $\text{N} \cdots \text{O}$ distances falling in the range 2.69(2)–3.13(3) Å. The sulfonate groups bridge *adjacent* $[\text{Ni}(\text{L}^2)_2]^{2+}$ units to form a two-dimensional polymeric array (see SI) rather than a simple 2:1 assembly of the type shown in Fig. 3(a).

The mutual perpendicularity of the tridentate ligands in the pseudo-octahedral complex $[\text{Ni}(\text{L}^2)_2]^{2+}$ leads to a separation and orientation of the terminal pyrazole NH groups that will not allow *intramolecular* H-bond bridging by a sulfonate unit as in Fig. 3(a). This conclusion is supported by the distances observed between the hydrogen atoms of *cis*-NH groups in the

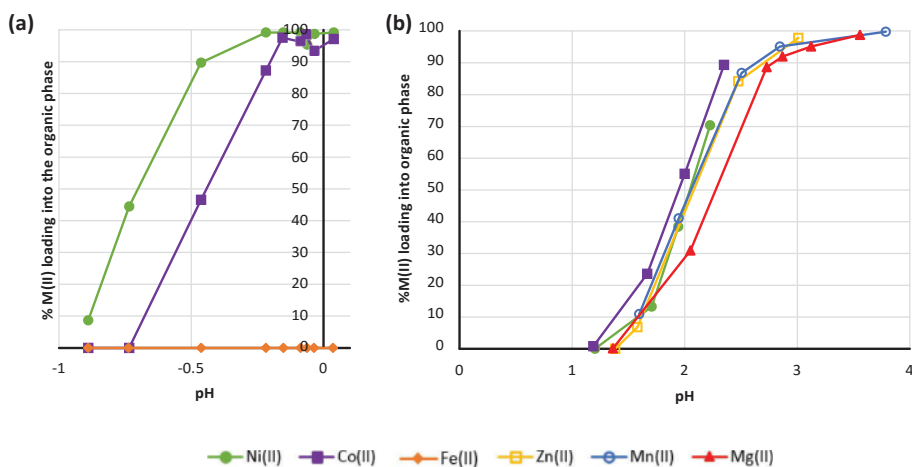


Figure 4. pH dependence of uptake of Fe(II), Co(II), and Ni(II) by (a) a CHCl_3 solution of DNNSAH (0.03 M) and L^1 (0.03 M) from an aqueous solution of their sulfate salts (each metal at 0.1 g L^{-1}) compared with (b) uptake by DNNSAH alone.^[44,47]

$[\text{Ni}(\text{L}^2)_2]^{2+}$ units in the well-defined structure of $[\text{Ni}(\text{L}^2)_2 \cdot (\text{ClO}_4)_2] \cdot \text{H}_2\text{O} \cdot \text{MeOH}$ (see Fig. 5) and in $[\text{Ni}(\text{bpp})_2]_2[\text{Cr}(\text{C}_2\text{O}_4)_3]\text{ClO}_4 \cdot 6\text{H}_2\text{O}$ ^[49] and $[\text{Ni}(\text{bppCF}_3)_2](\text{CF}_3\text{CO}_2)_2 \cdot \text{H}_2\text{O}$,^[50] where bpp and bppCF_3 are the unsubstituted and trifluoromethyl-substituted ligands 2,6-bis-(pyrazol-3-yl)pyridine and 2,6-bis-(5-trifluoromethylpyrazol-3-yl)pyridine, respectively. These distances fall in the range 4.63–5.69 Å. In $[\text{Ni}(\text{L}^2)_2 \cdot (\text{ClO}_4)_2] \cdot \text{H}_2\text{O} \cdot \text{MeOH}$, the water and methanol molecules use H-bonds to form bridges between pyrazole NH groups and perchlorate ions, reinforcing the three-dimensional structure.

Formation of *polynuclear* assemblies, $[\text{Ni}(\text{L}^1)_2 \cdot (\text{DNNSA})_2]_n$, when Ni is extracted by mixtures of L^1 and DNNSAH is consistent with the slow approach to equilibrium loading reported by Zhou *et al.*,^[43] as well as the relatively slow rates of exchange of water molecules in $\text{Ni}(\text{H}_2\text{O})_6^{2+}$ complexes.^[51] In this work, using chloroform as the diluent, equilibrium for the loading and stripping of Ni was achieved within 3 min. Nevertheless, electrospray mass spectrometry of solutions of $[\text{Ni}(\text{L}^2)_2 \cdot (2\text{-naphth-SO}_3)_2]$ in $\text{MeOH}/\text{CHCl}_3$ provides evidence for the presence of oligomeric assemblies (spectra are supplied in Section 3 of the ESI). The tetranuclear dication $[\text{Ni}_4(\text{L}^2)_6 \cdot (2\text{-naphth-SO}_3)_6]^{2+}$ is the most intense peak observed, followed by the mononuclear cation $[\text{Ni}(\text{L}^2)_2 \cdot (2\text{-naphth-SO}_3)]^+$.

Building simple molecular models of Ni-complexes of the *bidentate* ligands L^{3-7} in Table 1 reveals that the disposition of the pyrazole NH groups in neutral assemblies of generic formula $[\text{NiL}_3 \cdot (\text{DNNSA})_2]$ is much better suited to the formation of intramolecular H-bonds to sulfonate groups than that in the *tridentate* analogues L^1 and L^2 . X-ray crystal structures of $[\text{Ni}(\text{L}^3)_3 \cdot (2\text{-naphth-SO}_3)_2] \cdot \text{Et}_2\text{O}$ and $[\text{Ni}(\text{L}^7)_3 \cdot (2\text{-naphth-SO}_3)_2]$, which can be considered models for the possible assemblies formed by the extractants L^4 , L^5 , and L^6 , support this. A remarkably symmetrical set of six hydrogen bonds is found in the assembly $[\text{Ni}(\text{L}^7)_3 \cdot (2\text{-naphth-SO}_3)_2]$ (see Fig. 6), with $\text{NH} \cdots \text{O}$ distances falling in the range 1.93(3)–2.09(3) Å and $\text{N-H} \cdots \text{O}$ angles in the range 154(3)–168(4)°. With the exception of the naphthalene groups, the assembly has pseudo three-fold symmetry, very similar to that shown in Fig. 3(b). Its hydrophobic *t*-butyl and 2-naphthyl groups are located on the exterior of the assembly, suggesting that the *n*-nonyl-substituted extractant L^6 will be particularly well suited to transferring Ni(II) into a hydrocarbon diluent.

The monopyrazolyl ligand L^3 has just one NH group and, consequently, there are only three strong H-bond donor groups in $[\text{Ni}(\text{L}^3)_3]^{2+}$ to address the six sulfonate oxygen atoms in the $[\text{Ni}(\text{L}^3)_3 \cdot (2\text{-naphth-SO}_3)_2]$ assembly. The *mer*-isomer observed in the crystal structure of $[\text{Ni}(\text{L}^3)_3 \cdot (2\text{-naphth-SO}_3)_2] \cdot \text{Et}_2\text{O}$ (Fig. 7) has the two sulfonates located over opposed faces of the octahedron. One forms a strong H-bond to a pyrazole NH group, (N3 in Fig. 7) and two much weaker interactions to hydrogen atoms attached to carbon atoms (C2 and C3 in Fig. 7) on pyridine

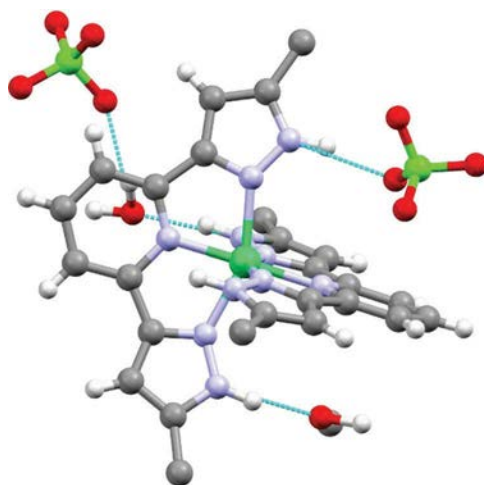


Figure 5. Asymmetric unit of the solid-state structure of $[\text{Ni}(\text{L}^2)_2][\text{ClO}_4]_2 \cdot \text{H}_2\text{O} \cdot \text{MeOH}$ showing the H-bonds formed by the pyrazole NH groups to perchlorate anions and water and methanol molecules. For clarity, the methyl groups of the *t*-butyl groups have been omitted.

units in the other two ligands (see table inset in Fig. 7). The other sulfonate forms two strong H-bonds, with HN1 and HN2, and one weak interaction with a pyridine H atom attached to C1 in Fig. 7. Whilst the three sulfonate-to-CH interactions are likely to be, at best, only very weakly bonding, they will contribute to stabilizing the ion-pairing and would help to reduce the exposure of the polar sulfonate groups to the nonpolar solvents used in solvent extraction.

The solid-state structures of the model compounds $[\text{Ni}(\text{L}^3)_3 \cdot (2\text{-naphth-SO}_3)_2]$ and $[\text{Ni}(\text{L}^7)_3 \cdot (2\text{-naphth-SO}_3)_2]$ suggest that ligands that facilitate H-bonding to the sulfonate groups in the *outer* coordination sphere would favor the formation of Ni complexes in solution in nonpolar solvents. However, when comparing the relative strengths of extractants that can facilitate such H-bonding with those that cannot, it is important to consider how the variations in structure will also influence the bonding in the *inner* coordination sphere. A comparison of the inner coordination spheres of $[\text{Ni}(\text{L}^2)_2 \cdot (2\text{-naphth-SO}_3)_2]$, $[\text{Ni}(\text{L}^2)_2][\text{ClO}_4]_2 \cdot \text{H}_2\text{O} \cdot \text{MeOH}$, $[\text{Ni}(\text{bpp})_2]_2[\text{Cr}(\text{C}_2\text{O}_4)]\text{ClO}_4 \cdot 6\text{H}_2\text{O}$,^[49] $[\text{Ni}(\text{L}^3)_3 \cdot (2\text{-naphth-SO}_3)_2] \cdot \text{Et}_2\text{O}$, and $[\text{Ni}(\text{L}^7)_3 \cdot (2\text{-naphth-SO}_3)_2]$ (see Tables 4 and 5) reveals that the bidentate nature of Motif B–D ligands in Table 1, L^{3-7} , allows them to form more nearly octahedral geometry around the Ni atom than found in complexes of the tridentate, Motif A, ligand. The bond angle variance values (σ_{oct} , the mean of the deviation of all the *cis*-angles in the octahedron from the ideal value of 90° , as defined in Eq. (1)) provides a measure of the distortion of an octahedral donor set.^[52] For the Ni(II) complexes of the bidentate ligands (Motifs B–D), these σ_{oct} values fall in the range $7.3\text{--}8.2$ compared with $10.6\text{--}11.1^\circ$ for complexes of the tridentate (Motif A) ligands. The large deviation of the $\text{N}_{\text{pyrazole}}\text{--Ni--N}_{\text{pyrazole}}$ angles from the ideal value of 180° recorded in Table 4 can be seen in Fig. 5. The distortion imposed by the tridentate ligands is also manifest by the significantly shorter $\text{N}_{\text{pyridine}}\text{--Ni}$ distances, $2.004(5)\text{--}2.006(5)$ Å, in $[\text{Ni}(\text{L}^2)_2][\text{ClO}_4]_2 \cdot \text{H}_2\text{O} \cdot \text{MeOH}$ and $[\text{Ni}(\text{bpp})_2]_2[\text{Cr}(\text{C}_2\text{O}_4)]\text{ClO}_4 \cdot 6\text{H}_2\text{O}$,^[49] than those found in $[\text{Ni}(\text{L}^3)_3 \cdot (2\text{-naphth-SO}_3)_2] \cdot \text{Et}_2\text{O}$, $2.099(3)\text{--}2.139(3)$ Å.

$$\sigma_{\text{oct}}^2 \approx \frac{1}{12} \sum_{i \neq j} \delta\sigma_{ij}^2 \quad (1)$$

The structural information on the model compounds discussed above, despite being obtained in the solid state, provides some insight into the factors that might influence the stability of assemblies formed in the water-immiscible solvents in extraction experiments. However, care needs to be taken when relating these

Table 4. Comparison of the coordination geometries in the $[\text{Ni}(\text{L})_2]^{2+}$ units of complexes of the tridentate (Motif A) ligands: 2,6-bis-(5-*t*-butylpyrazol-3-yl)pyridine (L^2), 2,6-bis-(5-trifluoromethylpyrazol-3-yl)pyridine (bppCF_3),^[50] and 2,6-bis-(pyrazol-3-yl)pyridine (bpp).^[49]

	$[\text{Ni}(\text{L}^2)]_2(\text{ClO}_4)_2 \cdot \text{H}_2\text{O} \cdot \text{MeOH}$	$[\text{Ni}(\text{bppCF}_3)_2](\text{CF}_3\text{CO}_2)_2 \cdot \text{H}_2\text{O}$	$[\text{Ni}(\text{bpp})_2]_2[\text{Cr}(\text{C}_2\text{O}_4)]\text{ClO}_4 \cdot 6\text{H}_2\text{O}^a$	
			A	B
Range of bond lengths/Å				
Ni-N _{pyridine}	2.004(5)–2.006(5)	2.004(4)–2.005(4)	2.022–2.029	2.005–2.007
M–N _{pyrazole}	2.081(6)–2.138(5)	2.094(4)–2.123(3)	2.086–2.121	2.085–2.155
Range of bond angles/°				
Intraligand	77.0(2)–77.3(3)	76.48(2)–77.1(2)	76.0–77.1	76.9–78.3
cis-N–Ni–N				
Interligand	86.0(2)–107.4(3)	89.4(2)–106.1(3)	91.3–107.5	91.7–104.7
cis-N–Ni–N				
Intraligand	152.6(2)–152.8(2)	153.4(2)–154.0(2)	153.0–153.8	154.5–155.1
trans-N–Ni–N				
Interligand	176.6(2)	176.8(2)	175.0	177.0
trans-N–Ni–N				
Bond angle variance ^b				
$\sigma_{\text{oct}}^\circ$	10.9	11.0	11.1	10.6

^aThe structure has two crystallographically independent complexes per unit cell.

^b σ_{oct} provides a measure of the distortion of an octahedral donor set,^[52] see Eq. (1).

Table 5. Comparison of the coordination geometries in the $[\text{Ni}(\text{L})_2]^{2+}$ units of complexes containing the bidentate synergistic ligands L^3 and L^7 .

	$[\text{Ni}(\text{L}^3)]_3(\text{naphth-SO}_3)_2$	$[\text{Ni}(\text{L}^7)]_3(\text{naphth-SO}_3)_2$
Range of bond lengths/Å		
Ni–N _{pyrazole}	2.057(2)–2.090(2)	2.086(3)–2.139(3)
Ni–N _{pyridine}	2.078(2)–2.122(2)	_{-^a}
Range of bond angles/°		
cis-N–Ni–N _{intraligand}	78.03(7)–78.68(6)	76.9(1)–77.4(1)
cis-N–Ni–N _{interligand}	89.24(7)–97.97(7)	89.7(1)–98.61(1)
trans-N–Ni–N _{interligand}	168.27(7)–172.05(6)	160.6(1)–170.7(1)
Bond angle variance ^b		
$\sigma_{\text{oct}}^\circ$	7.3	8.2

^aAll N-donors are in pyrazole units.

^b σ_{oct} provides a measure of the distortion of an octahedral donor set,^[52] see Eq. (1).

to the $\text{pH}_{1/2}$ data presented in Table 1, because they were determined in different diluents with different concentrations of extractants. Nevertheless, they are consistent with the proposition that simpler, lower-cost bidentate analogues of 2,6-bis-[5-*n*-nonylpyrazol-3-yl]pyridine,^[43] such as L^4 , L^5 , L^6 , and L^{9-11} , can be used as synergists for DNNSAH to generate very strong extractants for nickel. The pyrazolylpyridine reagents (Motif B, L^4 , and L^5 in Table 1) are stronger synergists for the extraction of Ni(II) and Co(II) (see Fig. 8) than L^1 and are more selective, potentially offering stepwise separation of these cations from Fe(II) and Zn(II).

The observation that the $\text{pH}_{1/2}$ values for the pyrazolyl synergists (L^1 and L^{4-6}) that contain NH groups are lower (Table 1) than those for the imidazole synergists (L^{9-11}), which do not, supports the proposition that the formation of $\text{NH} \cdots \text{O}_3\text{S}$ H-bonds of the types revealed in the solid-state structures (Figs. 6 and 7) favors Ni extraction by providing an additional source of stabilization to “electrostatic” ion-pairing in $[\text{NiL}_3 \cdot (\text{naphthalenesulfonate})_2]$ assemblies. However, if this were the only factor responsible for the relative strengths of the synergistic mixtures, we would expect the bispyrazole synergist L^6 , which can form six strong $\text{NH} \cdots \text{O}_3\text{S}$ H-bonds (see Fig. 6), to be more effective than the pyrazolylpyridine L^5 , which can only form three (see Fig. 7). The possibility that weak $\text{CH} \cdots \text{O}_3\text{S}$ bonding interactions may be formed by the latter and that the binding strengths of

	N...O / Å	H...O / Å	N-H...O / °
N1-H...O1	2.819(4)	2.01(3)	159(4)
N3-H...O2	2.871(4)	2.08(3)	154(3)
N2-H...O3	2.820(4)	2.02(3)	158(4)
N6-H...O4	2.833(4)	2.02(4)	161(4)
N4-H...O5	2.905(4)	2.09(3)	160(4)
N5-H...O6	2.773(4)	1.93(3)	168(4)

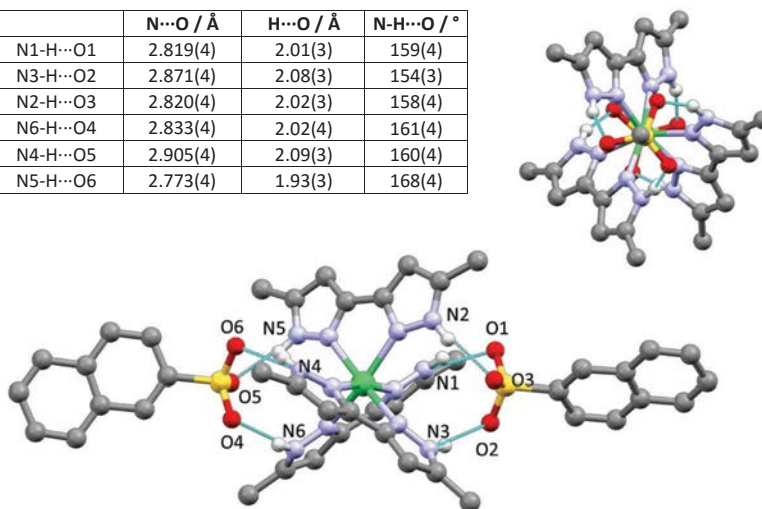
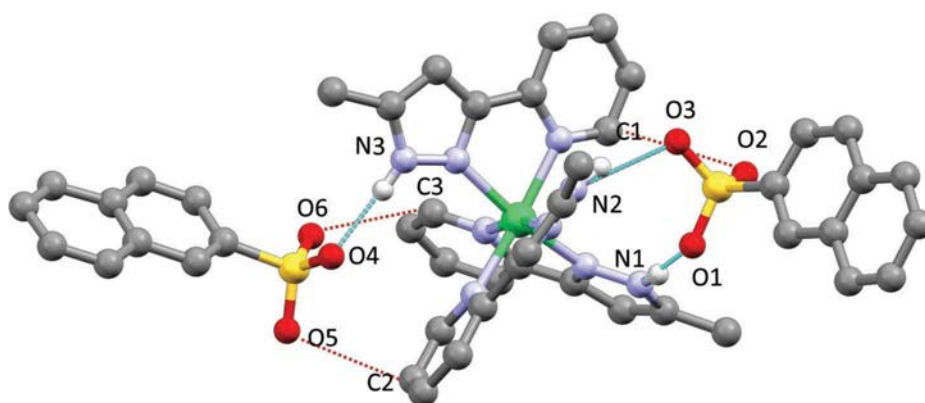


Figure 6. X-ray crystal structure of $[\text{Ni}(\text{L}^3)_3 \cdot (2\text{-naphth-SO}_3)_2]$ assembly showing the six pyrazole $\text{NH}\cdots\text{O}$ sulfonate H-bonds (on the left) and the pseudo three-fold symmetry (on the right). For clarity, the methyl groups of the *t*-butyl groups and H-atoms attached to carbon (and, on the right, all but the ipso C atom of the naphthalene units) have been omitted.



X-H...O	X...O / Å	H...O / Å	X-H...O / °
N1-H...O1	2.740(2)	1.80(3)	172(4)
C1-H...O2	3.954(3)	3.23(3)	104(3)
N2-H...O3	2.765(3)	1.95(3)	161(3)
N3-H...O4	2.782(2)	1.93(3)	174(3)
C2-H...O5	3.209(3)	2.92(4)	99(3)
C3-H...O6	3.090(3)	2.58(3)	113(3)

Figure 7. X-ray crystal structure of the $[\text{Ni}(\text{L}^3)_3 \cdot (2\text{-naphth-SO}_3)_2]$ assembly, showing the three pyrazole $\text{NH}\cdots\text{O}$ sulfonate H-bonds and the three pyridine $\text{CH}\cdots\text{O}$ contacts. Lengths and angles are provided in the inset table. H-atoms were inserted in calculated positions in the final stages of refinement and, for clarity, are not shown in the figure.

the bidentate ligands may differ as a consequence of differences in the nature of their nitrogen donor atoms are also likely to influence extraction strength.

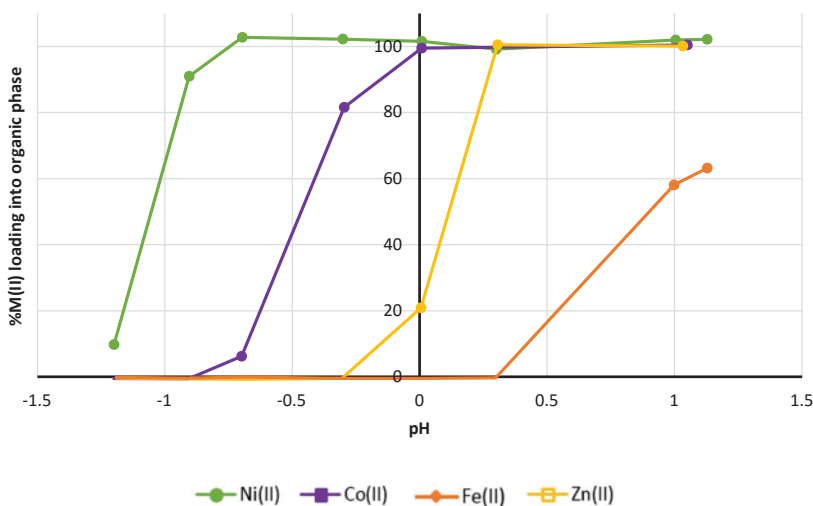


Figure 8. pH dependence of uptake of Fe(II), Co(II), Ni(II), and Zn(II) by a CHCl_3 solution of DNNSAH (0.04 M) and L^5 (0.06 M) from an aqueous solution of their sulfate salts (each metal at 0.1 g L^{-1}).

A further level of complexity in synergistic extraction of Ni(II) by DNNSAH lies in the extent to which inner-sphere water molecules are replaced when the metal is transferred to the water-immiscible phase. Okewole *et al.*^[44] found that 2,2'-pyridyl-1H-imidazole, PIMH, which has the structure shown in Table 1 (Motif D, R = H), forms a 2:1 complex with Ni(II) in ethanol/water (formulated as $[\text{Ni}(\text{PIMH})_2]\text{SO}_4 \cdot 4\text{H}_2\text{O} \cdot \frac{1}{2}\text{EtOH}$), but its electronic spectrum is consistent^[53] with the presence of the six-coordinate dication $[\text{Ni}(\text{PIMH})_2(\text{H}_2\text{O})_2]^{2+}$.

For the very strong synergists studied in this work (Motifs A, B, and C), evidence points to all of the inner-sphere water molecules being replaced by the bidentate ligands in the extraction process. Electronic spectra of loaded organic phases are consistent with the presence of an octahedral complex with an N_6 donor set.^[53] For example, the spectrum of a solution of $[\text{Ni}(\text{L}^2)_2 \cdot (2\text{-naphth-SO}_3)_2]$ in CHCl_3 (ESI, section 4), closely matches those of extensively studied $[\text{Ni}(\alpha\text{-di-imine})_3]^{2+}$ complexes^[54] and has its lowest energy band (the ${}^3\text{A}_{2g}$ to ${}^3\text{T}_{2g}$ transition) centered at 864 cm^{-1} , a value that suggests that the pyridinopyrazole L^2 is a slightly weaker field ligand than 2,2'-bipyridine.^[55]

Based on the observations above and the report by Okewole *et al.*, which was published^[44] whilst this work was being carried out, it is clear that bidentate nitrogen ligands containing unsaturated heterocycles can act as strong synergists for Ni extraction by DNSSAH. Consequently, an extensive range of comparable ligands (L^{12} – L^{39} in Table 2) was prepared and screened as synergists.

The screening reveals that ligands with the structural motifs shown in Fig. 9(a) are particularly strong synergists for Ni extraction by DNSSAH, giving $\text{pH}_{1/2}$ values below zero. As noted above, it is not appropriate to make subtle quantitative comparisons between the $\text{pH}_{1/2}$ data presented in Tables 1 and 2, because these have been determined in different diluents with different concentrations of extractants. Nevertheless, some striking structure/activity relationships are apparent. Five of the strongest synergists have NH groups adjacent to a nitrogen donor atom (Motifs B, C, E, and F in Fig. 9) or very close to it (Motif G). This is consistent with arguments presented above that H-bonding of such NH groups to the sulfonate oxygen atoms of DNSSA^- stabilizes assemblies formed in the organic phase. Motifs with comparable structures but having the NH unit replaced by a group having no H-bond donor properties are much weaker synergists. Examples of such weak synergists (Motifs J, M, and N in Fig. 9(b)) are otherwise structurally similar to the strong synergists with Motifs B, E, and F. The most notable exceptions to this rule of thumb are ligands L^{21} , L^{25} , L^{27} , and L^{34} , which have the Motifs I, L,

a. Strong synergists		
Motifs B, E, F	Motif C	Motif G
Motif I	Motif L	Motif Q
b. Weaker synergists with structures similar to Motifs B, E, and F		
Motif J	Motif M	Motif N

Figure 9. Generic structures of (a) the strongest synergists listed in Tables 1 and 2 compared with those of (b) structurally related much weaker synergists.

and Q (see Fig. 9(a)). It is possible that the N=CH unit in the five-membered rings in Motifs I and Q has a sufficiently polarized C–H bond that this can form weakly bonding interactions with sulfonate oxygen atoms. Examples of such C–H···O interactions were found in the X-ray structures described above.

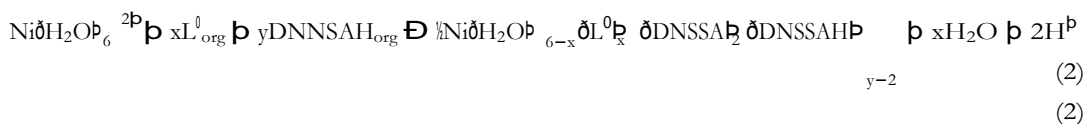
Conclusions

The program of synthesis and testing described above has demonstrated that many *bidentate* N-heterocycles that are structurally related to the previously reported^[42] *tridentate* synergist for DNNSAH extraction of Ni(II) (2,6-bis-[5-*n*-nonylpyrazol-3-yl]pyridine, L¹) can greatly enhance the strength and selectivity of nickel recovery. The strongest synergists, those with structural Motifs B and C in Table 1, contain pyrazole NH groups; X-ray crystal structures of model systems suggest that these can form strong H-bonds to the oxygen atoms of the DNNSA⁻ counteranion. This stabilizes the [Ni(L)₃·(DNSSA)₂] assemblies by complementing the ion-pairing forces and creates structures in which all the polar functional groups are shielded from a hydrophobic diluent.

The wide range of pH_{1/2} values afforded by using one of the new synergists, or of the previously reported^[14] reagents, is such that formulations could be devised to meet the requirements of many laterite-processing circuits (see Introduction). The strong pyrazole-containing synergists (Motifs B and C in Table 1) provide high selectivity and should allow a clean separation of Ni(II) from Co(II). Their chemical composition also makes them much more resistant to degradation by hydrolysis or oxidation than the oxime-containing synergists that have been previously tried.

For the most effective synergists described in this article, the mode of action involves displacement of all inner-sphere water molecules from the hydrated Ni²⁺ cation by bidentate nitrogen heterocycles. In contrast, for many of the long-established synergists^[56] for DNNSAH, coordinated water is retained in the extracted species. The generic equation (2), in which L' represents a monodentate ligand, defines the unusually wide range of modes of action of extraction that can be shown by DNNSAH. These are consequences of the sulfonate group being a very weak ligand and, as

far as we are aware, there is no evidence for extracted Ni complexes containing coordinated DNNSA⁻.



In assemblies such as $[\text{Ni}(\text{H}_2\text{O})_{6-x}(\text{L}')_x \cdot (\text{DNSSA})_2 \cdot (\text{DNSSAH})_{y-2}]$, both the acidic and conjugate anionic forms of the extractant could form H-bonds with the OH groups of water or with H-bond donors in the synergists, L'. This, and the strength of binding of the synergists to the Ni²⁺ or other cations in a feed solution, needs to be taken into account in predicting which synergists will be strong and selective reagents for Ni(II) and Co(II) recovery from laterites. Computational work is in hand^[57,58] to establish the relative importance of binding strengths in the inner and outer spheres of the M(II) species in developing synergists for DNSSAH and other acidic extractants.

Acknowledgments

We thank Solvay S.A., Anglo American, and University of Edinburgh's Principal's Career Development Scholarship scheme for the funding for PhD studentships for JWR, MRH, and EDD, respectively, James Cumby for discussions on the refinement of structure $[\text{Ni}(\text{L}')_2 \cdot (2\text{-naphth-SO}_3)_2] \cdot n\text{CHCl}_3$, and Furahi Achebe and Efrén Delos Santos (Solvay) for technical assistance in the synthesis of many of the candidate synergists. Discussions with Violina Griffin (Solvay) are gratefully acknowledged.

References

- [1] Elias, M.; Nickel Laterite Deposits: Geological Overview, Resources and Exploitation. In *Giant Ore Deposits: Characteristics, Genesis and Exploration*; Cooke, D., Pongratz, J., Eds.; Centre for Ore Deposit Research, University of Tasmania: Hobart, Tasmania, 2002. pp. 205–220.
- [2] US Geological Survey, Mineral Commodity Summary, Nickel, 112, <https://minerals.usgs.gov/minerals/pubs/mcs/2018/mcs2018.pdf> (Jan, 2018).
- [3] Biley, C. A.; Pelsler, M.; den Hoed, P.; Hove, M.; Development of the Iron-Focused Laterite (ARFe) Process. In *Southern African Base Metals Conference*, Southern African Institute of Mining and Metallurgy, Johannesburg, 2013, pp. 169–178.
- [4] Mudd, G. M.; Global Trends and Environmental Issues in Nickel Mining: Sulfides versus Laterites. *Ore Geol. Rev.* 2010, 38(1–2), 9–26. DOI: 10.1016/j.oregeorev.2010.05.003.
- [5] Crundwell, F.; Moats, M.; Ramachandran, V.; Robinson, T. Davenport W. G.; In *Extractive Metallurgy of Nickel, Cobalt and Platinum Group Metals*, Chapter 1, Elsevier: Oxford, 2011.
- [6] Moskalyk, R. R.; Alfantazi, A. M.; Nickel Laterite Processing and Electrowinning Practice. *Miner. Eng.* 2002, 15(8), 593–605. DOI: 10.1016/S0892-6875(02)00083-3.
- [7] Reid, J. G.; Laterite Ones-Nickel and Cobalt Resources for the Future. *Nickel '96 Mineral to Market*; Australasian Institute of Mining and Metallurgy: Victoria, Australia, 1996.
- [8] Suttill, K. R.; Colombia - Coal, Gold, Emeralds, and Much Else. *Eng. Min. J.* 1994, 195, 5, 29–40.
- [9] Reid, J. G.; Queensland Nickel-Value Added Products from Technological Advances. *Proceedings of the Australasian Institute of Mining and Metallurgy Annual Conference*. Canberra, Australia, 1995. pp. 131–135.
- [10] Donegan, S.; Direct Solvent Extraction of Nickel at Bulong Operations. *Miner. Eng.* 2006, 19, 12, 1234–1245.
- [11] Sole, K. C.; Cole, P. M.; Purification of Nickel by Solvent Extraction. In *Ion Exchange and Solvent Extraction. A Series of Advances*; Marcus Y., SenGupta A. K., Eds.; Marcel Dekker: New York, 2002; Vol. 15, pp. 143–195.
- [12] Mihaylov, I.; Krause, E.; Colton, D. F.; Okita, Y.; Duterge, J. P.; Perraud, J. J.; The Development of a Novel Hydrometallurgical Process for Nickel and Cobalt Recovery from Goro Laterite Ore. *CIM Bulletin*, 2000, 93 (1041), 124–130.
- [13] Ichlas, Z. T.; Ibane, D. C.; Process Development for the Direct Solvent Extraction of Nickel and Cobalt from Nitrate Solution: Aluminum, Cobalt, and Nickel Separation Using Cyanex 272. *Int. J. Miner. Metall. Mater.* 2017, 24(1), 37–46. DOI: 10.1007/s12613-017-1376-7.
- [14] Cheng, C. Y.; Barnard, K. R.; Zhang, W.; Robinson, D. J.; Synergistic Solvent Extraction of Nickel and Cobalt: A Review of Recent Developments. *Solvent Extr. Ion Exch.* 2011, 29(5–6), 719–754. DOI: 10.1080/07366299.2011.595636.
- [15] Preston, J. S.; du Preez, A. C.; Synergistic Effects in the Solvent Extraction of Some Divalent Metals by Mixtures of Versatic 10 Acid and Pyridinecarboxylate Esters. *J. Chem. Technol. Biotechnol.* 1994, 61(2), 159–165. DOI: 10.1002/(ISSN)1097-4660.

- [16] Preston, J. S.; du Preez, A. C.; The Solvent Extraction of Nickel from Acidic Solutions Using Synergistic Mixtures Containing Pyridinecarboxylate Esters. *J. Chem. Biochem. Tech.* **1994**, *66*, 295–299.
- [17] Preston, J. S.; du Preez, A. C.; Separation of Nickel and Calcium by Solvent Extraction Using Mixtures of Carboxylic Acids and Alkylpyridines. *Hydrometallurgy* **2000**, *58*(3), 239–250. DOI: 10.1016/S0304-386X(00)00135-3.
- [18] Preston, J. S.; Solvent Extraction of Nickel and Cobalt by Mixtures of Carboxylic Acids and Non-Chelating Oximes. *Hydrometallurgy* **1983**, *11*(1), 105–124. DOI: 10.1016/0304-386X(83)90019-1.
- [19] Preston, J. S.; du Preez, A. C. Synergistic Effects in Solvent-Extraction System Based on Alkylsalicylic Acids. Part 2. Extraction of Nickel, Cobalt, Cadmium and Zinc in the Presence of Some Neutral N-, O- and S-Donor Compounds. *Solvent Extr. Ion Exch.* **1996**, *14*(2), 179–201. DOI: 10.1080/07366299608918334.
- [20] Preston, J. S.; du Preez, A. C.; Solvent Extraction of Nickel from Acidic Solutions Using Synergistic Mixtures Containing Pyridinecarboxylate Esters. Part 1. Systems Based on Organophosphorus Acids. *J. Chem. Technol. Biotechnol.* **1996**, *66*(1), 86–94. DOI: 10.1002/(ISSN)1097-4660.
- [21] Cheng, C. Y.; Urbani, M. D.; Davies, M. G.; Pranolo, Y.; Zhu, Z.; Recovery of Nickel and Cobalt from Leach Solutions of Nickel Laterites Using a Synergistic System Consisting of Versatic 10 and Acorga CLX 50. *Miner. Eng.* **2015**, *77*, 17–24. DOI: 10.1016/j.mineng.2015.01.015.
- [22] Zhang, W.; Pranolo, Y.; Urbani, M.; Cheng, C. Y.; Extraction and Separation of Nickel and Cobalt with Hydroxamic Acids LIX1104, LIX1104SM and the Mixture of LIX1104 and Versatic 10. *Hydrometallurgy* **2012**, *119-120*, 67–72. DOI: 10.1016/j.hydromet.2012.02.012.
- [23] Turner, N. L.; Barnard, K. R.; The Effect of Individual Complexed Metals on Hydroxyoxime Stability in the LIX 63 - Versatic 10 - Tributyl Phosphate Synergistic Solvent Extraction System under Synthetic Nickel Laterite Extract Conditions. *Hydrometallurgy* **2012**, *117-118*, 79–85. DOI: 10.1016/j.hydromet.2012.02.006.
- [24] Barnard, K. R.; Turner, N. L.; Hydroxyoxime Stability and Unusual Cobalt Loading Behaviour in the LIX 63- Versatic 10-Tributyl Phosphate Synergistic System under Synthetic Laterite Conditions. *Hydrometallurgy* **2011**, *109*(1-2), 29–36. DOI: 10.1016/j.hydromet.2011.05.004.
- [25] Barnard, K. R.; Turner, N. L.; Reagent Stability in Synergistic SX Systems Incorporating LIX® 63 Oxime and Versatic 10, Part 3: Nickel Laterite Case Study. In *Proc. International Solvent Extraction Conference*, Tucson, Arizona: Metallurgical Society of CIM, **2008**, pp. 909–914.
- [26] Barnard, K. R.; Turner, N. L.; The Effect of Temperature on Hydroxyoxime Stability in the LIX 63- Versatic 10-Tributyl Phosphate Synergistic Solvent Extraction System under Synthetic Nickel Laterite Conditions. *Hydrometallurgy* **2011**, *109*(3-4), 245–251. DOI: 10.1016/j.hydromet.2011.07.010.
- [27] Du Preez, R.; Kotze, M.; Nel, G.; Donegan, S.; Masiwa, H.; Solvent Extraction Test Work to Evaluate a Versatic 10/Nicksyn[™] Synergistic System for Nickel-Calcium Separation. In *Fourth Southern African Conference on Base Metals*, Southern African Institute of Mining and Metallurgy, Johannesburg, **2007**, pp. 193–210.
- [28] Masiwa, H.; Mathe, O.; Donegan, S.; Nel, G.; du Preez, R.; Kotze, M.; Ireland, N.; Evaluation of Versatic 10 and Versatic 10/Nicksyn[™] Synergistic Systems for Nickel-Calcium Separation on the Tati BMR Hydrometallurgical Demonstration Plant. In *International Solvent Extraction Conference*, Tucson, Arizona: Metallurgical Society of CIM, **2008**, pp. 169–175.
- [29] Du Preez, A. C.; Preston, J. S.; Separation of Nickel and Cobalt from Calcium, Magnesium and Manganese by Solvent Extraction with Synergistic Mixtures of Carboxylic Acids. *J. South. African Inst. Min. Metall.* **2004**, *104*, 6, 333–338.
- [30] Du Preez, A. C.; Kotze, M. H.; Evaluation of a Versatic 10 acid/Nicksyn[™] Synergistic System for the Recovery of Nickel and Cobalt from a Typical Lateritic Leach Liquor. In *Base Metals Conference*, Southern African Institute of Mining and Metallurgy, Johannesburg, **2013**, pp. 193–208.
- [31] Steyl, J. D. T.; Pelsler, M.; Smit, J.; Atmospheric Leach Process for Nickel Laterite Ores. In *Sixth International Symposium*, Young C. A., Taylor, P., Anderson, C. G., Choi Y. Eds.; Society for Mining, Metallurgy, and Exploration, Inc.: Littleton, Colorado, **2008**, pp. 541–550.
- [32] Barnard, K. R.; Nealon, G. L.; Ogden, M. I.; Skelton, B. W.; Crystallographic Determination of Three Ni- α -Hydroxyoxime-Carboxylic Acid Synergist Complexes. *Solvent Extr. Ion Exch.* **2010**, *28*(6), 778–792. DOI: 10.1080/07366299.2010.515169.
- [33] Smit, J. T.; Steyl, J. D. T.; Leaching Process in the Presence of Hydrochloric Acid for the Recovery of a Value Metal from an Ore. **2006**; Int. Patent No. WO 2006/043158.
- [34] Smit, J. T.; Steyl, J. D. T.; Pelsler, M.; Process for the Recovery of Metals from an Iron-Containing Ore. **2011**; Int. Patent No. WO 2011/015991 A2.
- [35] Jones, D. L.; Mayhew, K.; Mean, R.; Neef, M.; Unlocking Disseminated Nickel Sulphides Using the CESL Nickel Process. In *ALTA 2010 Nickel-Cobalt Conference*, ALTA Metallurgical Services, Melbourne, **2010**.
- [36] Schlesinger, M. E.; King, M.; Sole, K. C.; Davenport, W.; *Extractive Metallurgy of Copper*, 5th ed.; Elsevier: Amsterdam, Netherlands., **2011**.
- [37] Sole, K. C.; Zarate, G.; Steeples, J.; Tinkler, O.; Robinson, T. G.; Global Survey of Copper Solvent Extraction Operations and Practices. In *Copper-Cobre 2013 Conference*, Santiago, Chile: Geccamin, **2013**, pp. 137–148.
- [38] Robinson, T. G.; Sole, K. C.; Sandoval, S.; Moats, M.; Siegmund, A.; Davenport, W. E.; Copper Electrowinning – 2013 World Operating Tankhouse Data. In *Copper-Cobre 2013 Conference*, Santiago, Chile: Geccamin, **2013**, pp. 3–14.

- [39] Moser, M.; *Private Communication, Solvay-Cytec*; Stamford, USA, 2017.
- [40] United Nations Conference on Trade and Development Multi-Year Expert Meeting on Commodities and Development 2013. http://unctad.org/meetings/en/Presentation/SUC_MYEM2013_20032013_Don%20SMAL.E.pdf.
- [41] Edelstein, D. L.; Porter, K. D.; *Copper Statistics 1900-2008*; United States Geological Survey: Washington, DC, USA, 2010.
- [42] Zhou, T.; and Pesic, B.; A Pyridine-Based Chelating Solvent Extraction System for Selective Extraction of Nickel and Cobalt. *Hydrometallurgy* 1997, 46, 1–2, 37–53.
- [43] Grinstead, R. R.; Extraction of Copper, Nickel and Cobalt Using Alkylaromatic Sulfonic Acids and Chelating Amines. 1981; US Patent No. 4,254,087.
- [44] Okewole, A. I.; Magwa, N. P.; Tshentu, Z. R.; The Separation of Nickel(II) from Base Metal Ions Using 1-Octyl- 2-(2'-Pyridyl)Imidazole as Extractant in a Highly Acidic Sulfate Medium. *Hydrometallurgy* 2012, 121-124, 81– 89. DOI: 10.1016/j.hydromet.2012.04.002.
- [45] Still, W. C.; Kahn, M.; Mitra, A.; Rapid Chromatographic Technique for Preparative Separations with Moderate Resolution. *J. Org. Chem.* 1978, 43(14), 2923–2925. DOI: 10.1021/jo00408a041.
- [46] Roebuck, J. W.; Sassi, T.; Fischmann, A. J.; Griffin, V.; Tasker, P. A.; Aliphatic-Aromatic Heterocyclic Compounds and Uses Thereof in Metal Extractant Compositions. 2016; Int. Patent No. WO2016160168 A1.
- [47] Fleming, J. S.; Psillakis, E.; Couchman, S. M.; Jeffery, J. C.; McCleverty, J. A.; Ward, M. D.; Complexes of the Potentially Hexadentate Ligand Bis{3-[6-(2,2'-Bipyridyl)]Pyrazol-1-Yl}Hydroborate with Representative S-, P-, D- and F-Block Metal Ions: Factors Promoting Formation of Mononuclear or Double-Helical Dinuclear Complexes. *J. Chem. Soc. Dalt. Trans.* 1998, 4, 537–544. DOI: 10.1039/a707936b.
- [48] Osseo-Asare, K.; Zheng, Y. Solubilization and Metal Complexation in a Reversed Micellar Hydroxyoxime—Sulfonic Acid Liquid—Liquid Extraction System. *Colloids and Surfaces* 1991, 53(2), 339–347. DOI: 10.1016/0166-6622(91)80146-F.
- [49] Coronado, E.; Giménez-López, M. C.; Gimenez-Saiz, C.; Martínez-Agudo, J. M.; Romero, F. M.; Synthesis, Structure and Magnetic Properties of Iron (II), Cobalt (II) and Nickel (II) Complexes of 2,6-Bis(Pyrazol-3-Yl)Pyridine and Paramagnetic Counterions. *Polyhedron* 2003, 22(14–17), 2375–2380. DOI: 10.1016/S0277-5387(03)00242-0.
- [50] Khmara, E. F.; Chizhov, D. L.; Sidorov, A. A.; Aleksandrov, G. G.; Slepukhin, P. A.; Kiskin, M. A.; Tokarev, K. L.; Filyakova, V. I.; Rusinov, G. L.; Smolyaninov, I. V.; Bogomyakov, A. S.; Starichenko, D. V.; Shvachko, Y. N.; Korolev, A. V.; ; et al. Synthesis, Structure, Electrochemical and Magnetic Properties of 2,6-Bis(5-Trifluoromethylpyrazol-3-Yl)Pyridine and Its Ni(II) Complexes. *Russ. Chem. Bull.* 2012, 61(2), 313–325.
- [51] Purcell, K. F.; Kotz, J. C.; *Inorganic Chemistry*; Holt-Saunders: London, UK, 1977.
- [52] Robinson, K.; Gibbs, G. V.; Ribbe, P. H.; Quadratic Elongation: A Quantitative Measure of Distortion in Coordination Polyhedra. *Science (80-)*. 1971, 172(3983), 567–570. DOI: 10.1126/science.172.3983.567.
- [53] Drago, R. S.; *Physical Methods in Inorganic Chemistry*; Rheinhold: New York, NY, 1967.
- [54] Robinson, M. A.; Curry, J. D.; Busch, D. H.; Complexes Derived from Strong Field Ligands. XVII. Electronic Spectra of Octahedral Nickel(II) Complexes with Ligands of the α -Diimine and Closely Related Classes. *Inorg. Chem.* 1963, 2(6), 1178–1181. DOI: 10.1021/ic50010a021.
- [55] Jørgensen, C. K.; Smith, L. H.; Hanshoff, G.; Prydz, H.; Comparative Crystal Field Studies of Some Ligands and the Lowest Singlet State of Paramagnetic Nickel(II) Complexes. *Acta Chem. Scand.* 1955, 9, 1362–1377. DOI: 10.3891/acta.chem.scand.09-1362.
- [56] Li, J.; Hu, H.; Zhu, S.; Hu, F.; Wang, Y.; The Coordination Structure of the Extracted Nickel(II) Complex with a Synergistic Mixture Containing Dinonylnaphthalene Sulfonic Acid and 2-Ethylhexyl 4-Pyridinecarboxylate Ester. *Dalt. Trans.* 2017, 46(4), 1075–1082. DOI: 10.1039/C6DT04369K.
- [57] Healy, M. R.; PhD thesis, Outer-Sphere Interactions in Metal Solvent Extraction Systems, University of Edinburgh, Edinburgh, UK, 2016.
- [58] Nicolson, R. M.; *Unpublished Work*; University of Edinburgh: Edinburgh, UK, 2017.